Atmos. Meas. Tech. Discuss., 5, 2363–2393, 2012
www.atmos-meas-tech-discuss.net/5/2363/2012/
doi:10.5194/amtd-5-2363-2012

Atmospheric Measurement Techniques Discussions

Assessment of diverse algorithms applied on MODIS Aqua and Terra data over land surfaces in Europe

P. Glantz and M. Tesche

Department of Applied Environmental Science, Stockholm University, Stockholm, Sweden

Received: 8 March 2012 – Accepted: 9 March 2012 – Published: 19 March 2012

Correspondence to: P. Glantz (paul.glantz@itm.su.se)

Published by Copernicus Publications on behalf of the European Geosciences Union.

Abstract

The aim of the present study is to validate AOT (aerosol optical thickness) and Ångström exponent (α), obtained with the SAER (Satellite AErosol Retrieval) algorithm for MODIS (MODerate resolution Imaging Spectroradiometer) Aqua and Terra calibrated level 1 data (1 km horizontal resolution at ground) and MODIS Collection 5 (c005) standard product retrievals (10 km), against AERONET (AErosol RObotic NETwork) observations over land surfaces in Europe. The three time periods investigated in this study have been chosen to enable a validation of the algorithm for a maximal possible variation in sun elevations. For several of the cases analyzed here the Aqua and Terra satellites passed the investigation area twice during a day. Thus, beside a variation in the sun elevation the satellite retrievals have also on a daily basis been performed with a significant variation in the satellite-viewing geometry. An inter-comparison of the two algorithms has also been performed. The validation with AERONET shows that the MODIS c005 retrieved AOT is, for the wavelengths 0.469 and 0.500 nm, on the whole within the expected uncertainty for one standard deviation of the MODIS c005 retrievals over Europe ($\Delta\text{AOT} = \pm 0.05 \pm 0.15\,\text{AOT}$). The SAER estimated AOT for the wavelength 0.443 nm also agree reasonable well with AERONET. Thus, the majority of the SAER AOT values are within the MODIS expected uncertainty range, although somewhat larger root mean square deviation occurs compared to the results obtained with the MODIS c005 algorithm. The discrepancy between SAER and AERONET AOT is, however, substantially larger for the wavelength 488 nm, which means that the values are to a large extent outside of the expected MODIS uncertainty range. Both satellite retrieval algorithms are unable to estimate α accurately, although the MODIS c005 algorithm performs better. Based on the inter-comparison of the SAER and MODIS c005 algorithms it was found that the SAER is able to obtain results within the expected uncertainty range of MODIS for Aqua and Terra observations during periods 1 and 3. The same was found for MODIS Aqua observations during period 2 but only for AOT below 0.5.

AMTD

5, 2363–2393, 2012

1 Introduction

Beside an increase in greenhouse gases human activities have lead to a perturbation of the atmospheric content of aerosol particles (IPCC, 2007). Aerosols exhibit a high spatial and temporal variability in the atmosphere. Therefore, studies on the effect of aerosols on climate and measures for environmental control require an accurate identification of aerosol sources and distributions, their strength, and the released aerosol type. Such information can be retrieved from space-borne observations. Several contemporary satellite-borne radiometers have produced data for aerosol investigations during the last decade. To estimate the impact of aerosols on climate aerosol optical thickness (AOT) is a useful parameter, since it can be applied in radiative transfer calculations and evaluation of the treatment of aerosols in regional and climate models. However, since the radiance at the top-of-atmosphere (TOA) detected by the satellite sensors are not only caused by aerosols in the atmosphere and has to be related to the AOT the satellite retrievals are not a straightforward task. Therefore, beside development of algorithms for satellite retrievals high priority should be given to validating the corresponding results of aerosol optical properties against ground-based remote sensing data. Results of remote sensing observations from different space-borne platforms as well as with different sensors mounted on the same satellite need be evaluated. In a recent paper, Mishchenko et al. (2010) have evaluated AOT, retrieved from data obtained with the Multi-angle Imaging SpectroRadiometer (MISR, Kahn et al., 2005) and MODerate resolution Imaging Spectroradiometer (MODIS, Remer et al., 2008), against data obtained with ground-based sun photometers by the AErosol RObotic NETwork (AERONET, Holben et al., 1998). MISR and MODIS are both mounted situated aboard the NASA Earth Observing System's Terra spacecraft and scan the Earth's surface in a polar orbit. The agreement of ground- and satellite-based AOT presented by Mishchenko et al., (2010) is far less favorable than what has been obtained in previous studies (e.g., Kahn et al., 2006, 2009; Liu et al., 2004; Remer et al., 2008). Kahn et al. (2011) suggest that the reasons for these discrepancies can be explained to

AMTD
5, 2363–2393, 2012

a large extend by the analysis approach applied by Mishchenko et al. (2010) that (in comparison to the earlier studies) differs in (1) the treatment of outliers, (2) the application of absolute versus relative criteria for testing agreement, and (3) the ways in which seasonally varying spatial distributions of coincident retrievals are taken into account. Kahn et al. (2011) furthermore criticize that Mishchenko et al. (2010) do not distinguish between observational sampling differences and retrieval algorithm error.

As another point, the evaluation of satellite aerosol retrievals should also account for the diversity of algorithms that are currently in use. Kokhanovsky et al. (2010) compare several major aerosol retrieval algorithms by using a synthetic data set of TOA radiation for a model atmosphere and under the assumption of a black surface. In this way, the assumptions made in the different aerosol models that are incorporated in the various algorithms could be investigated. One important conclusion of this study is that accurate aerosol retrievals need to include more discrete aerosol models.

The aim of the present study is to validate AOT and the Ångström exponent (α), obtained with the somewhat modified Bremen Aerosol Retrieval (BAER) algorithm (von Hoyningen-Huene et al., 2003, 2011), which will hereafter be referred to as Satellite AErosol Retrieval (SAER), and MODIS collection 5 (c005) standard aerosol products (Remer et al., 2008) against AERONET observations over land surfaces in Europe. Findings of the SAER retrievals are furthermore compared to MODIS c005 for all Terra and Aqua scenes included in this study. In previous studies BAER has been applied to satellite data obtained by the Medium Resolution Imaging Sensor (MERIS), Sea-viewing Wide Field Sensor (SeaWiFS) and MODIS (e.g., von Hoyningen-Huene et al., 2006, 2011; Glantz et al., 2009a,b). The present algorithm is applied on calibrated level 1 data, which means that the column aerosol optical properties are estimated according to a high spatial resolution (0.3–1 km) at ground. Hence, this algorithm has a good development potential also to be used in urban air quality studies (Treffeisen et al., 2007; Glantz et al., 2009a). Even so, Von Hoyningen-Huene et al. (2006) and Glantz et al. (2009a) found that AOT retrieved with BEAR from MODIS Aqua and MERIS data was lower than AERONET observations for high aerosol loading and approximately

AMTD
5, 2363–2393, 2012

a factor of 2 higher for low aerosol loading. From an inter-comparison between BAER MODIS Aqua and BAER MERIS Glantz et al. (2009a) also suggests a bias in AOT for situations with differences in the elevation of the sun. The latter caused by a difference in the overpasses of the satellites with approximately 1 h. However, differences in the viewing angle between the two satellite sensors could as well contribute to observed discrepancy in AOT. Even so, by introducing a surface bi-directional reflectance distribution function (BRDF) in combination with an air mass corrected reflectance von Hoyningen-Huene et al. (2011) found a better agreement between MERIS and AERONET. Note however that the MERIS scenes are associated with a relatively narrow swath width. Since the MODIS scenes are substantially broader means that the present SAER algorithm has here been validated for situations with a larger variation in the satellite viewing geometry compared to aerosol retrievals based on MERIS data. The time periods investigated in this study have been chosen to enable a validation of the algorithm for a maximal possible variation in sun elevations.

2 Data retrievals, data sources and methods

2.1 Satellite nadir viewing retrieval

The MODIS observations considered in this study were performed at various sun elevations. MODIS is a nadir-viewing instrument on a sun-synchronous near-polar orbit. The instrument scans the Earth's surface 90° left and right to the ground-track and produces scenes with a swath width of 2330 km at ground. For comparison, MERIS scenes only have a swath width of 1150 km. Consequently, beside the elevation of the sun MODIS aerosol retrievals are also highly dependent on the viewing angle of the sensor, which varies between 0° and ∼ 65° (0° to ∼ 40° for MERIS). Since MODIS produces relatively broad satellite scenes two overpasses occurred over the AERONET stations for some of the days investigated here. The local equatorial crossing time is approximately 10:30 a.m. (descending node) and 01:30 p.m. local time (ascending node) for Terra and

AMTD
5, 2363–2393, 2012

Aqua, respectively. Hence, the sun-zenith/satellite-viewing geometry between the two platforms is expected to differ on daily basis.

2.1.1 SAER algorithm

The SAER algorithm has been used to retrieve AOT from TOA radiances measured with the nadir-viewing sensor MODIS over land surfaces. MODIS measures upwelling or TOA radiance (I_{TOA}) as well as the solar extraterrestrial irradiance (E_0) at visible and near infrared wavelengths. Normalization of I_{TOA} to the solar illumination conditions for each wavelength λ results in the TOA-reflectance ρ_{TOA}:

$$\rho_{TOA}(\lambda, \theta_0, \theta_s, \phi) = \frac{\pi \cdot I_{TOA}}{E_0 \cdot \cos(\theta_0)} \quad (1)$$

where θ_0 and θ_s are the solar zenith and satellite viewing angles, respectively, and Φ is the azimuth angle.

The retrieval of AOT relies on the representation of ρ_{TOA} and solution of the radiative transfer equation for the aerosol reflectance ρ_{Aer} (Kaufman et al., 1997; von Hoyningen-Huene et al., 2003, 2006):

$$\rho_{Aer}(\lambda, \theta_0, \theta_s, \phi) = \rho_{TOA}(\lambda, \theta_0, \theta_s, \phi) - \rho_{TOA}(\lambda, \theta_0, \theta_s, \phi) - \frac{T_{Ray}(\lambda, M(\theta_0)) \cdot T_{Ray}(\lambda, M(\theta_s)) \cdot T_{Aer}(\lambda, M(\theta_0)) \cdot T_{Aer}(\lambda, M(\theta_s)) \cdot A_{Surf}(\lambda, \theta_0, \theta_s, \phi)}{1 A_{Surf}(\lambda, \theta_0, \theta_s, \phi) \cdot \rho_{Hem}(\lambda, \theta_0)} \quad (2)$$

where ρ_{Ray} is the path reflectance of the Rayleigh scattering. T_{Ray} and T_{Aer} both represent the total (direct and diffuse) and direct atmospheric transmission. M is the air mass factor and ρ_{Hem} is the hemispheric reflectance. T_{Ray} and ρ_{Hem} are determined by parameterizations as derived from radiative transfer calculations (von Hoyningne-Huene et al., 2006). For the determination of AOT, a surface reflectance A_{Surf} is estimated based on a mixing model of green vegetation (ρ_{Veg}) and bare soil (ρ_{Soil}) spectra:

$$A_{Surf}(\lambda) = F \cdot [C_{Veg} \cdot \rho_{Veg}(\lambda) + (1 - C_{Veg}) \cdot \rho_{Soil}] \quad (3)$$

AMTD
5, 2363–2393, 2012

with:

$$C_{\mathrm{Veg}} = \mathrm{NDVI} = \frac{\rho_{\mathrm{TOA}}(0.858\,\mu\mathrm{m}) - \rho_{\mathrm{TOA}}(0.645\,\mu\mathrm{m})}{\rho_{\mathrm{TOA}}(0.858\,\mu\mathrm{m}) - \rho_{\mathrm{TOA}}(0.645\,\mu\mathrm{m})} \tag{4}$$

where NDVI used as a proxy for the vegetation fraction and the scaling factor F for the level of the surface reflectance determinate at 0.645 µm:

$$F = \frac{\rho_{\mathrm{TOA}}(0.645) - \rho_{\mathrm{Ray}}(0.645)}{C_{\mathrm{Veg}} \cdot \rho_{\mathrm{Veg}}(0.645) + \left(1 - C_{\mathrm{Veg}}\right) \cdot \rho_{\mathrm{Soil}}(0.645)}. \tag{5}$$

Similar to the work by von Hoyningen-Huene et al. (2011), an air-mass corrected aerosol reflectance factor

$$\rho_{\mathrm{Aer\_ac}} = \rho_{\mathrm{Aer}} \frac{0.5 \cdot M(z_0) + 1.5 \cdot M(z_{\mathrm{s}})}{M(z_0)^{0.5} \cdot M(z_{\mathrm{s}})^{1.5}} \tag{6}$$

has been introduced, although weighted in the present case to account for the larger MODIS viewing angle compared to MERIS. This factor should be considered as preliminary since it is still under investigation.

Finally, AOT is determined according to look-up-tables (LUTs) that describe the relationship between aerosol reflectance and AOT. The LUTs were obtained by radiative transfer calculations performed with aerosol phase functions measured during the LACE-98 experiment (von Hoyningen-Huene et al., 2003) and a single scattering albedo of 1. The latter parameter represents non-absorbing aerosols. The transmission parameters in Eq. (2) are dependent on AOT. In a first iteration AOT is calculated based on Rayleigh transmissions only. Later in the process, the iteration converges and stops when the difference between the AOT values used in the estimation of the transmission parameter and the one obtained according to the LUT is lower than 0.01. The Ångström exponent

$$\alpha = \frac{\ln \frac{\tau_{\lambda_1}}{\tau_{\lambda_2}}}{\ln \frac{\lambda_1}{\lambda_2}} \tag{7}$$

AMTD
5, 2363–2393, 2012

is calculated for the wavelength pair 443 and 665 nm (Ångström, 1964). This parameter is commonly used to characterize the wavelength dependence of AOT and to provide some basic information on aerosol size (Eck et al., 1999).

A cloud screening approach has been included in the present work. First, a pixel is interpreted as a thick cloud if $\rho_{TOA} > 0.2$ (Kokhanovsky, 2006). Second, pixels having a ratio of AOT (443 nm)/AOT (469 nm) < 1.08 between the blue channels are considered as thin clouds due to their significantly reduced Rayleigh scattering component. Third, in order to exclude pixels associated with inhomogeneous clouds the variability within a 3 × 3 pixel masque has been investigated. If the ratio between one standard deviation and mean AOT (for values higher than 0.2) is lower than 0.1 the grid box is assumed to be cloud-free. For mean AOT values equal or lower than 0.2 the threshold of the ratio is higher and has been set to 0.3.

2.1.2 MODIS c005 algorithm

In the present study we use the MODIS c005 level 2 standard aerosol products for retrievals over land surfaces with relatively low surface reflection ("dark target"). Data has been taken from the NASA Goddard Space Flight Center's Atmosphere Archive and Distribution System (http://ladsweb.nascom.nasa.gov). A detailed description of the MODIS c005 algorithm can be found in Levy et al. (2010), although some features of the method are described here. The MODIS algorithm uses two visible channels (0.469 and 0.645 µm) and one near infrared band (2.1 µm). Note that a vegetated surface is not "dark" at the green wavelength and therefore the MODIS visible channels cannot be used directly. The near infrared band shows almost no absorption and scatter from gases and aerosols, respectively, but is highly sensitive to surface reflection. Based on the latter and that a consistent spectral relationship occurs over vegetated land surface (Kaufman et al., 1997) the surface reflection at the wavelengths 0.469 and 0.645 µm can be estimated. Wavelengths in other parts of the spectrum are used to mask out non-dark-target conditions, such as deserts as well as snow and ice surfaces (Ackerman et al., 1998; Li et al., 2005). A single scattering albedo of 0.95 that

AMTD
5, 2363–2393, 2012

represents weakly absorbing aerosols is used for the area investigated (Europe). The MODIS level 2 aerosol product represents AOT on a 10 km grid. The spectral observations occur however according to a horizontal resolution of 500 m and are screened for clouds (Gao et al., 2002; Martins et al., 2002). The pixels that remain in the 10 km box are sorted according to their relative reflectance (at 0.66 µm) and 20 % and 50 % of the darkest and brightest pixels, respectively, are removed. This means that at most 120 pixels and at least 12 pixels (3 %) remain from the original 400. The remaining pixels are averaged to one set of spectral reflectances that is used to retrieve aerosol products representing $10 \times 10\,\mathrm{km}^2$ boxes. The AOT for the wavelengths 459 and 645 nm are used for the calculation of α according to Eq. (7).

2.1.3 Comparison of SAER and MODIS c005

A pixel by pixel comparison of the AOT retrieved with SAER and obtained by MODIS c005 was performed in the framework of this study. For this, the findings obtained with SAER were averaged to match the MODIS c005 resolution of $10 \times 10\,\mathrm{km}^2$. After this, the coefficient of determination (R^2), the average absolute deviation (AAD), and the relative AAD were determined for collocated pixels of the satellite scenes by means of a linear regression. The AAD and relative AAD are defined as

$$\mathrm{AAD} = \sum_{i=1}^{N} \frac{\mathrm{abs}\,[x_i - \bar{x}]}{N} \tag{8}$$

and

$$\mathrm{relAAD} = \frac{\mathrm{AAD}}{\left[\mathrm{MODIS}\ \overline{\mathrm{AOT}} + \mathrm{BAER}\ \overline{\mathrm{AOT}}/2\right]} \tag{9}$$

AMTD
5, 2363–2393, 2012

where

$$x_i = \text{MODIS AOT}_i - \text{SAER AOT}_i, \quad i = 1, ..., N$$

$$\bar{x} = \frac{1}{N} \sum_{i=1}^{N} x_i. \tag{10}$$

The index i refers to collocated MODIS and SAER pixels with the total number N of such pairs. Particularly when performing satellite retrievals of aerosol optical properties over land, large outliers are expected (Kahn et al., 2011). The AAD does not weights larger outliers to the same degree as the root mean square deviation (RMSD) and therefore this statistical approach seems more appropriate in the present comparison of the two satellite algorithms. In the comparison between satellite retrievals and AERONET observations however the RMSD has been calculated.

2.2 AOT from AERONET sun photometers

The satellite retrievals of AOT have been validated against AERONET level 2.0 (quality assured) data obtained at Belsk (51.84° N, 20.79° E), Cabauw (51.97° N, 4.93° E), Dunkerque (51.04° N, 2.37° E), Hamburg (53.57° N, 9.97° E), Ispra (45.80° N, 8.63° E), Karlsruhe (49.09° N, 8.43° E), Laegeren (47.48° N, 8.35° E), Leipzig (51.35° N, 12.44° E), Minsk (53.92° N, 27.60° E), Munich (48.15° N, 11.57° E), SMHI (Swedish meteorology and hydrology institute, 58.58° N, 16.15° E), and Toravere (58.26° N, 26.46° E). The locations of these sites are shown in Fig. 1. Information about the Cimel sun photometers operated at these sites can be found at http://aeronet.gsfc.nasa.gov. AERONET data used for the present study include AOT at 440 and 500 nm as well as α (440/675 nm). These values were recorded every 15 min and automatically cloud screened. AERONET derived estimates of spectral AOT are expected to be accurate within ±0.02 (e.g., Holben et al., 1998).

AMTD
5, 2363–2393, 2012

3 Results of AOT over Europe

The satellite aerosol optical properties have been investigated over Europe for three time periods; 1 to 10 May 2006 (period 1), 1 to 14 July 2006 (period 2) and 26 March to 1 April 2007 (period 3). Periods 1 and 3 were both influenced by high pressure systems, estimated by the European Centre for Medium-Range Weather Forecasts (ECMWF), with cores mainly located over Finland and Eastern Ukraine/Southern Russia, respectively. Such a weather situation favors the accumulation of aerosols from local sources but also enables long-range transport of from the east. To get an impression of the conditions during the periods under investigation Fig. 2 shows visible composites from MODIS observations for days corresponding to the three periods. The example days suggest that more clouds were present during period 2 compared to periods 1 and 3. This is also valid when the full periods are considered (not shown). Additionally, aerosols generated from agricultural fires in Ukraine and Russia highly influenced the investigation area in Europe during periods 1 and 3 (Stohl et al., 2007 and Cook et al., 2008, respectively). Enhanced reflection of solar radiation by aerosols from these sources is visible in the cloud-free areas in the right and left parts of Fig. 3a,c, respectively.

3.1 Case study

Figure 3 shows 555-nm AOT retrieved with the SAER and MODIS c005 algorithms for two MODIS Aqua overpasses over Europe at 10:45 and 12:20 UTC on 1 April 2007. The enhanced AOT values shown in Fig. 3a,b are caused by aerosols from agricultural fires over Ukraine and Russia (Cook et al., 2008). The figures show that on the whole good agreement occurs between the results obtained by the two algorithms, particularly for areas associated with high aerosol loadings. The statistics shown in Fig. 3a confirm this. For lower aerosol loadings however the figures show that relatively large discrepancy in AOT occurs over some part of the investigation area; e.g. Southern Sweden and west of the Gulf of Finland. The enhanced values over the latter area

AMTD
5, 2363–2393, 2012

shown in Fig. 3a is probably influenced by clouds, which means that the SAER cloud screening fail for these satellite pixels.

Furthermore, AOT at 532 nm estimated by CALIPSO (Cloud Aerosol Lidar and Infrared Pathfinder Satellite Observations, Winker et al., 2003) according to four tracks over Europe for 1 April 2007 is shown in Fig. 1. On the whole similar values as the ones shown in Fig. 3a,b are obtained in areas associated both with high and low aerosol loadings, with the exception for southeast where MODIS classified the area as cloudy while CALIPSO estimate AOT values near 1. MODIS visible composite suggest that clouds actually are formed in this area. Note that a comparison of AOT from CALIPSO and MODIS should be considered as qualitative, since CALIPSO level 2 AOT is not intended for scientific use. Based on profiles created by CALIPSO in the area near Belsk extinction coefficient values of approximately 0.4 km^{-1} within a more or less constant layer from surface up to 2.3 km (not shown) are obtained. This gives an AOT value of about 0.9, which agree well with results obtained with the sun photometer at Belsk during this day, represented by the highest AERONET values (> 0.8) at 500 nm shown in Figs. 6e,f and 8e,f.

3.2 Validation against AERONET

For a comparison with AERONET data, findings from the two satellite retrievals were averaged over at most 9 cloud-free pixels adjacent to and including the pixel that corresponds to a ground site. This means that the SAER and MODIS c005 retrievals were averaged according to as largest an area of 10 and 100 km^2, respectively. AERONET measurements were averaged over a time period of 60 min centered with respect to the satellite overpasses. Mean values for a comparison were only considered if the averaging could be performed over at least two cloud-free satellite pixels and two AERONET AOT measurements. An overview of the mean number of satellite pixels and AERONET measurements included in comparison for the three time periods considered in this study is provided by Table 1. Generally, the number of pixels averaged for the satellite retrieval is close to the maximum number of 9. Slightly smaller values and a larger

AMTD
5, 2363–2393, 2012

deviation are found for Aqua overpasses, which occur closer to noon than Terra overpasses. Thus, the difference could in part be explained by an advanced mixing of the planetary boundary layer, which results in increased cloud formation during the later satellite overpasses. A comparison of MODIS visible composite pictures for the periods investigated (not shown) generally shows higher cloud cover for overpasses of Aqua compared to the ones of Terra.

3.2.1 MODIS c005 AOT and α

Figure 4 shows the result of the comparison of AOT, as retrieved with the MODIS c005 algorithm at 469 nm and measured at the AERONET stations (Fig. 1) at 440 nm during the present time periods. The comparison is separated according to MODIS measurements aboard the Aqua and Terra satellites. On the whole the AOT values are within the expected uncertainties of one standard deviation of the MODIS retrievals over land ($\Delta AOT = \pm 0.05 \pm 0.15 AOT$, Remer et al., 2008). The figure also shows that the largest relative RMSD (relRMSD) occurs for period 2, which is associated with larger cloud cover than the other two time periods. These findings confirm the high quality of the results of the MODIS c005 retrieval over dark land surface that was also found by Remer et al. (2008) for a global data set. Furthermore, high values of α as obtained from AERONET measurements (color coded in Figs. 4a,c,e) suggest a dominance of submicron aerosols over Europe during the periods investigated. However, Fig. 4 indicates that poor agreements are found between MODIS c005 α (469/645) and AERONET α (440/675), which is more clearly shown in Fig. 5, where comparisons of the absolute values are presented. This is probably due to even small errors in AOT amplify substantially in the calculation of α (Eq. 7).

The comparison presented in Fig. 4 was also performed for MODIS c005 and AERONET AOT at 555 and 500 nm, respectively. Though the MODIS wavelength is somewhat longer than the one belong to AERONET, the linear fits are very close to the 1-to-1 line shown in Fig. 6 for MODIS Aqua, periods 1 and 2, and for MODIS Terra, period 1.

AMTD
5, 2363–2393, 2012

3.2.2 SAER AOT and α

A comparison comparable to the one presented in the previous section is shown in Fig. 7 for AOT retrieved with SAER at 443 nm and measured with AERONET at 440 nm. Although relatively good agreement is found generally larger relRMSD values are shown in the figures compared to the results obtained with the operational MODIS algorithm. In addition, substantially lower and widespread values of α are obtained with SAER compared to AERONET. A comparison was also performed for SAER retrievals at 488 nm and AERONET measurements at 500 nm. Figure 8 shows that substantially larger discrepancy in AOT was found for these wavelengths compared to the comparison performed according to the blue wavelength. The larger deviation may mainly be due to the surface reflection that is higher for longer wavelength within the solar spectrum (von Hoyningen-Huene et al., 2003), which means that the estimation of AOT with the SAER approach is more sensitive here compared to the satellite retrievals at the blue wavelength.

3.3 Inter-comparison between SAER and MODIS

Figure 9 shows an inter-comparison of 469-nm AOT as retrieved with SAER and the operational MODIS c005 algorithm. To compile the figure, AOT derived with SAER was averaged according to the MODIS pixel resolution of $10 \times 10\,km^2$ (Sect. 2.1.2). Relatively good agreement is found between the two algorithms, although values of AOT obtained with SAER are systematically lower than the ones obtained with the MODIS algorithm for high aerosol loading. This can be seen particularly for Terra corresponding to period 2 (Fig. 9d). For AOT smaller than 1, results obtained with the SAER algorithm are well within the expected uncertainty of one standard deviation of the MODIS retrieval for both Aqua and Terra corresponding to periods 1 and 3. The same good agreement is also found for Aqua and period 2, but only for AOT values lower than 0.5. Part of the discrepancy that is obtained between SAER and MODIS c005 shown

AMTD
5, 2363–2393, 2012

in Fig. 9 could indeed be due to clouds that are not screen out correctly by the former algorithm (Sect. 3.1) for all satellite pixels that have been included in the present study.

3.4 Discussion

The inter-comparison of the findings of MODIS c005 and SAER retrievals and the validation of these algorithms against AERONET measurements suggests that a small part of the deviation found for high aerosol loadings may be due to a general overestimation of AOT by the operational MODIS algorithm. From the substantially larger RMSD for the comparison of findings of the SAER retrieval with AERONET measurements (Fig. 7) with respect to the one found for MODIS c005 and AERONET (Fig. 4), however, it can be concluded that a major part of the discrepancy presented in Fig. 9 is probably caused by uncertainties in the SAER approach. For a better view on this effect, Fig. 10a,b shows the comparison of the findings of the two algorithms for two single Terra overpasses at 09:00 and 10:40 UTC, respectively, on 1 April 2007. Areas of high aerosol loadings appear near the edge (overpass at 09:00) and middle (overpass at 10:40) of the satellite scenes for this day (not shown), simultaneously as a difference in the elevation of the sun and even larger disparity in the viewing angle appear (Sect. 2.1). Thus, the treatment of the sun zenith satellite viewing geometry in the SAER retrieval is most likely responsible for a major part of the discrepancy observed in Figs. 9 and 10 for situations with high aerosol loading. Additionally, the larger deviation that occurs between SAER and AERONET AOT at green wavelengths compared to blue wavelengths may be explained by a higher sensitivity of the satellite retrievals for lower wavelengths, particularly for low aerosol loadings. This is because the surface reflection increases substantially for longer wavelength within the solar spectrum (von Hoyningen-Huene et al., 2003). Poor agreement between SAER and AERONET was found for α. Poor agreement was also found between values of α obtained from MODIS c005 and AERONET, which is surprising since good agreement was found for the AOT retrieved with the two platforms at blue and green wavelengths. This is then probably

AMTD
5, 2363–2393, 2012

explained by uncertainties in the estimates of AOT at two different wavelengths that substantially increase in the calculation of α according to Eq. (7).

4 Summary and conclusions

Findings of AOT and α from satellite retrievals by the MODIS c005 and SAER algorithms, applied to data collected from the MODIS Aqua and Terra sensors over Europe, were inter-compared and validated against AERONET measurements for three periods in spring and summer. For several of the cases analyzed here the Aqua and Terra satellites passed the area investigated twice a day. Beside a variation in the sun elevation between the two overpasses, the satellite retrievals were also applied to scenes with a significant variation in the satellite-viewing geometry.

The validation with AERONET for sites in Central Europe shows that results of AOT obtained with the MODIS c005 algorithm, for the wavelengths 469 and 555 nm, were generally found to vary within the expected uncertainty for one standard deviation of the MODIS retrievals ($\Delta AOT = \pm 0.05 \pm 0.15\,AOT$). The AOT retrieved with the SAER algorithm for the wavelength of 443 nm also agrees reasonable well with AERONET. Thus the majority of the SAER values are also within the expected MODIS uncertainty range, although somewhat larger RMSD occurs compared to the MODIS c005 algorithm. The discrepancy between AOT derived with SAER at 488 nm and measured by AERONET at 500 nm is however substantially larger, thus, the former values are to a larger extent located outside of the expected MODIS uncertainty range. Both satellite retrieval algorithms are unable to estimate α accurately, although the MODIS c005 algorithm performs better.

Based on the inter-comparison of the results of the SAER and MODIS c005 algorithms it was found that SAER is able to obtain results within the expected uncertainty range of MODIS for Aqua and Terra observations during periods 1 and 3 as long as AOT does not exceed 1. The same was found for MODIS Aqua observations during period 2 but only for AOT below 0.5. The present results suggest that the deviation that

AMTD
5, 2363–2393, 2012

occurs between the two algorithms (i.e., values outside the MODIS expected uncertainty range), is most likely caused by the treatment of the sun-satellite viewing geometry in the SAER algorithm. The present study suggests that the air-mass correction of the column reflectance introduced as a factor in Eq. (5) needs further investigation. The same holds for the BRDF suggested by von Hoyningen-Huene et al. (2011), since its introduction did not lead to any improvement of the findings of the aerosol retrievals considered here. The present results suggest also that at least a small part of the discrepancies that occur between the two algorithms are caused by the SAER method used for the cloud screening.

It can be concluded from this study that satellite retrievals of AOT from MODIS measurements over Central Europe, particularly when obtained with the MODIS c005 algorithm, are of very high quality and thus can be used in the validation of regional and climate models. Note that the satellite scenes considered here covered a variety of aerosols from marine and continental sources in Europe but also from agricultural fires in Russia and Ukraine. The latter events were associated with high aerosol loadings and AOT beyond 1, although probably with a single scattering albedo similar to aerosols classified as clean. For the case study presented in Sect. 3.1, active remote sensing observations performed with the CALIPSO lidar were also considered, though not in terms of a detailed discussion. Such data can be used to gain information about the vertical aerosol distribution (i.e., profiles of the aerosol extinction coefficient) and are complementary to the column observations obtained with passive remote sensing. Future studies can provide a much more detailed view of the observed aerosol situation by using a combination of passive (AOT, α) and active (vertical distribution) remote sensing. Such comprehensive data sets furthermore provide a better foundation for the validation of the treatment of aerosols in regional and climate models than is the case when only using maps of column-integrated AOT.

Acknowledgement. We thank the PIs of the AERONET sites used in this study for maintaining their stations. We acknowledge the MODIS and CALIPSO mission scientists and associated NASA personnel for the production of the data used in this research effort. The authors are

AMTD
5, 2363–2393, 2012

also thankful for the use of ECMWF data sets. The work was financed through research grants from the Swedish Research Council for the Environment, Agricultural Sciences and Spatial Planning (FORMAS).

References

Ackerman, S. A., Strabala, K. L., Menzel, W. P., Frey, R. A., Moeller, C. C., and Gumley, L. E.: Discriminating clear sky from clouds with MODIS, J. Geophys. Res.-Atmos., 103(D24), 32141–32157, 1998.

Ångström, A.: The parameters of atmospheric turbidity, Tellus, 16, 64–75, 1964.

Cook, A., Willis, P., Webster, H., Harrison, M.: UK Air Quality Forecasting: a UK Particulate Episode from 24th March to 2th April 2007, Report AEAT/ENV/R/2566 Issue 1, AEA Technology plc, AEA Energy & Environment, Oxfordshire, UK, 2008.

Eck, T. F., Holben, B. N., Reid, J. S., Dubovik, O., Smirnov, A., O'Neill, N. T., Slutsker, I., and Kinne, S.: Wavelength dependence of the optical depth of biomass-burning, urban, and desert dust aerosols, J. Geophys. Res., 104, 31333–31349, doi:10.1029/1999JD900923, 1999.

Gao, B., Kaufman, Y. J., Tanre, D., and Li, R.: Distinguishing tropospheric aerosols from thin cirrus clouds for improved aerosol retrievals using the ratio of 1.38 µm and 1.24 µm channels, Geophys. Res. Lett., 29(18), 1890, doi:10.1029/2002GL015475, 2002.

Glantz, P., Johansson, C., Kokhanovsky, A., and von Hoyningen-Huene, W.: Estimating $PM_{2.5}$ over Southern Sweden using spaceborne optical measurements, Atmos. Environ., 43(36), 5838–5846, 2009a.

Glantz, P., Nilsson, D. E., and von Hoyningen-Huene, W.: Estimating a relationship between aerosol optical thickness and surface wind speed over the ocean, Atmos. Res., 92(1), 58–68, 2009b.

Holben, B. N., Eck, T. F., Slutsker, I., Tanré, D., Buis, J. P., Setser, A., Vermote, E., Reagan, J. A., Kaufman, Y. J., Nakajima, T., Lavenu, F., Jankowiak, I., and Smirnov, A.: AERONET – a federated instrument network and data archive for aerosol characterization, Remote Sens. Environ., 66, 1–16, 1998.

von Hoyningen-Huene, W., Freitag, M., and Burrows, J. B.: Retrieval of aerosol optical thickness over land surface from top-of-atmosphere radiance, J. Geophys. Res., 108(D9), 4260, 2003.

AMTD

5, 2363–2393, 2012

von Hoyningen-Huene, W., Kokhanovsky, A., Burrows, J. P., Bruniquel-Pinel, V., Regner, P., and Baret, F.: Simultaneous determination of aerosol- and surface characteristics from top-of-atmosphere reflectance using MERIS on board of ENVISAT, Adv. Space Res., 37, 2172–2177, 2006.

von Hoyningen-Huene, W., Yoon, J., Vountas, M., Istomina, L. G., Rohen, G., Dinter, T., Kokhanovsky, A. A., and Burrows, J. P.: Retrieval of spectral aerosol optical thickness over land using ocean color sensors MERIS and SeaWiFS, Atmos. Meas. Tech., 4, 151–171, doi:10.5194/amt-4-151-2011, 2011.

IPCC, 2007: Climate Change 2007: The Physical Science Basis, Contribution of Working Group I to the Fourth Assessment Report of the Intergovernmental Panel on Climate Change, edited by: Solomon, S., Qin, D., and Manning, M., Cambridge University Press, Cambridge, UK, 2001.

Mishchenko, M. I., Liu, L., Geogdzhayev, I. V., Travis, L. D., Cairns, B., and Lacis, A. A.: Toward unified satellite climatology of aerosol properties. 3. MODIS versus MISR versus AERONET, J. Quant. Spectr. Radiat. T., 111, 540–552, 2010.

Kahn, R. A., Gaitley, B. J., Martonchik, J. V., Diner, D. J., Crean, K. A., and Holben, B.: Multiangle imaging spectroradiometer (MISR) global aerosol optical depth validation based on 2 years of coincident aerosol robotic network (AERONET) observations, J. Geophys. Res., 110, D10S04, doi:10.1029/2004JD004706, 2005.

Kahn, R. A., Nelson, D. L., Garay, M. J., Levy, R. C., Bull, M. A., Diner, D. J., Martonchik, J. V., Paradise, S. R., Hansen, E. G., and Remer, L. A.: MISR aerosol product attributes, and statistical comparisons with MODIS, IEEE Trans. Geosci. Remote Sens., 47, 4095–4114, 2009.

Kahn, R. A., Garay, M. J., Nelson, D. L., Levy, R. C., Bull, M. A., Diner, D. J., Martonchik, J. V., Hansen, E. G., Remer, L., and Tanré, D.: Response to "Toward unified satellite climatology of aerosol properties. 3. MODIS versus MISR versus AERONET", J. Quant. Spectr. Radiat. T., 112, 901–909, 2011.

Kaufman, Y. J., Tanré, D., Gordon, H. R., Nakajima, T., Lenoble, J., Frouin, R., Grassl, H., Herman, B. M., King, M. D., and Teillet, P. M.: Passive remote sensing of tropospheric aerosol and atmospheric correction for the aerosol effect, J. Geophys. Res., 102, 16815–16830, 1997.

Kokhanovsky, A. A.: Cloud Optics, Springer, Dordrecht, 2006.

AMTD
5, 2363–2393, 2012

Kokhanovsky, A. A., Deuzé, J. L., Diner, D. J., Dubovik, O., Ducos, F., Emde, C., Garay, M. J., Grainger, R. G., Heckel, A., Herman, M., Katsev, I. L., Keller, J., Levy, R., North, P. R. J., Prikhach, A. S., Rozanov, V. V., Sayer, A. M., Ota, Y., Tanré, D., Thomas, G. E., and Zege, E. P.: The inter-comparison of major satellite aerosol retrieval algorithms using simulated intensity and polarization characteristics of reflected light, Atmos. Meas. Tech., 3, 909–932, doi:10.5194/amt-3-909-2010, 2010.

Levy, R. C., Remer, L. A., Kleidman, R. G., Mattoo, S., Ichoku, C., Kahn, R., and Eck, T. F.: Global evaluation of the Collection 5 MODIS dark-target aerosol products over land, Atmos. Chem. Phys., 10, 10399–10420, doi:10.5194/acp-10-10399-2010, 2010.

Li, R., Remer, L., Kaufman, Y., Mattoo, S., Gao, B., and Vermote, E.: Snow and ice mask for the MODIS aerosol products, IEEE Geosci. Remote S., 2(3), 306–310, 2005.

Liu, Y., Sarnat, J. A., Coull, B. A., Koutrakis, P., and Jacob, D. J.: Validation of MISR aerosol optical thickness measurements using Aerosol Robotic Network (AERONET) observations over the contiguous United States, J. Geophys. Res., 109, D06205, doi:10.1029/2003JD003981, 2004.

Martins, J., Tanre, D., Remer, L., Kaufman, Y., Mattoo, S., and Levy, R.: MODIS cloud screening for remote sensing of aerosols over oceans using spatial variability, Geophys. Res. Lett., 29(12), 1619, doi:10.1029/2001GL013252, 2002.

Remer, L. A., Kleidman, R. G., Levy, R. C., Kaufman, Y. J., Tanré, D., Mattoo, S., Martins, J. V., Ichoku, C., Koren, I., Yu, H., and Holben, B. N.: Global aerosol climatology from the MODIS satellite sensors, J. Geophys. Res., 113, D14S07, doi:10.1029/2007JD009661, 2008.

Stohl, A., Berg, T., Burkhart, J. F., Fjæraa, A. M., Forster, C., Herber, A., Hov, Ø., Lunder, C., McMillan, W. W., Oltmans, S., Shiobara, M., Simpson, D., Solberg, S., Stebel, K., Ström, J., Tørseth, K., Treffeisen, R., Virkkunen, K., and Yttri, K. E.: Arctic smoke – record high air pollution levels in the European Arctic due to agricultural fires in Eastern Europe in spring 2006, Atmos. Chem. Phys., 7, 511–534, doi:10.5194/acp-7-511-2007, 2007.

Treffeisen, R., Tunved, P., Ström, J., Herber, A., Bareiss, J., Helbig, A., Stone, R. S., Hoyningen-Huene, W., Krejci, R., Stohl, A., and Neuber, R.: Arctic smoke – aerosol characteristics during a record smoke event in the European Arctic and its radiative impact, Atmos. Chem. Phys., 7, 3035–3053, doi:10.5194/acp-7-3035-2007, 2007.

Winker, D. M., Vaughan, M. A., Omar, A., Hu, Y., Powell, K. A., Liu, Z., Hunt, W. H., and Young, S. A.: Overview of the CALIPSO mission and CALIOP data processing algorithms, J. Atmos. Oceanic Technol., 26, 2310–2323, 2009.

AMTD
5, 2363–2393, 2012

Table 1. Mean number and one standard deviation of satellite pixels and AERONET measurements, used to obtain the mean AOT and α values for the validation of the satellite retrievals with ground-based measurements for the three time periods considered in this study.

	1–10 May 2006	1–14 Jul 2006	26 Mar–1 Apr 2007
Satellite retrieval			
$SAER_{MODIS\ Aqua}$	8.25 ± 1.98	8.24 ± 1.97	8.82 ± 0.87
$SAER_{MODIS\ Terra}$	8.83 ± 1.05	8.76 ± 0.93	8.92 ± 0.49
$MODIS_{c005\ Aqua}$	8.32 ± 1.32	7.55 ± 2.26	8.48 ± 1.15
$MODIS_{c005\ Terra}$	8.46 ± 1.33	7.79 ± 2.01	8.25 ± 1.68
AERONET compared to			
Aqua	3.02 ± 1.22	3.38 ± 1.28	4.00 ± 1.07
Terra	3.59 ± 1.05	3.78 ± 1.06	3.82 ± 1.22

AMTD
5, 2363–2393, 2012

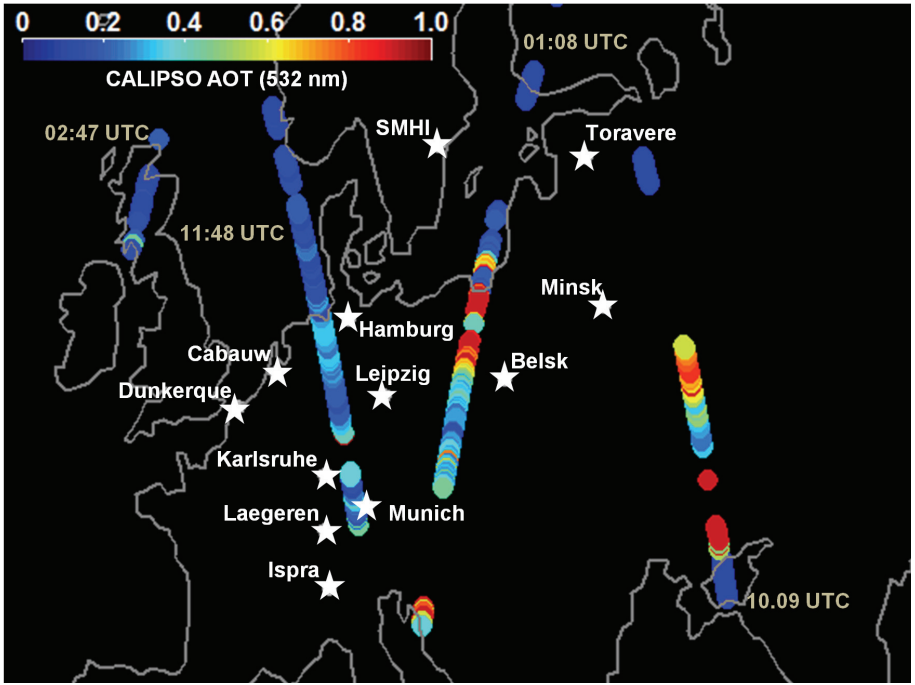

Fig. 1. Location of the AERONET stations used in the present study. The colored dots represent AOT at 532 nm as obtained from CALIPSO measurements during day and night tracks on 1 April 2007.

AMTD
5, 2363–2393, 2012

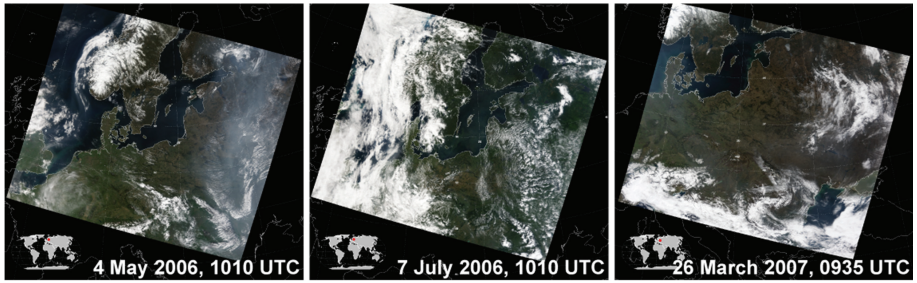

Fig. 2. MODIS visible composite pictures over Europe for **(a)** 4 May 2006, **(b)** 7 July 2006 and **(c)** 26 March 2007.

AMTD
5, 2363–2393, 2012

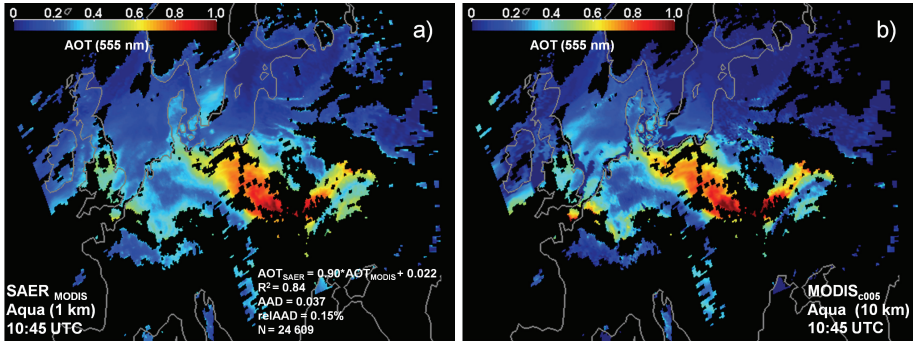

Fig. 3. Aqua satellite scenes of AOT at 555 nm over land and ocean surfaces in Europe for two overpasses at 10:45 and 12:20 UTC on 1 April 2007 obtained with **(a)** the SAER algorithm and **(b)** the MODIS c005 algorithm. Text at the right bottom in **(a)** gives the expression for the linear regression curve, R^2, AAD, relative AAD, and the number of collocations (N) of the linear regression between the results of the two algorithms for a pixel-by-pixel comparison.

AMTD
5, 2363–2393, 2012

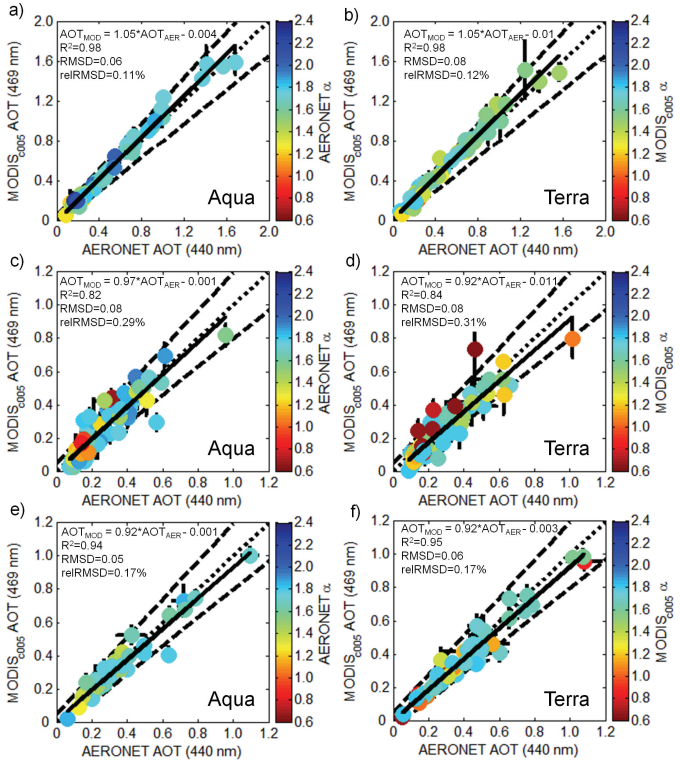

Fig. 4. Comparison between MODIS c005 and AERONET AOT at 469 and 440 nm, respectively, for Aqua (left column) and Terra (right column), and period 1 (top), 2 (middle) and 3 (bottom). The color code refers to α as obtained with AERONET and MODIS for the wavelength pairs 440/675 nm and 469/645 nm, respectively. The solid, dashed, and dotted lines represent linear fits of the AOT values (with bins of 0.05), expected uncertainties for one standard deviation of the MODIS c005 aerosol retrievals, and the 1-to-1 line, respectively. Text at the top describes the expression for the linear regression curve, coefficient of determination (R^2), root mean square deviation (RMSD) and relative RMSD.

AMTD
5, 2363–2393, 2012

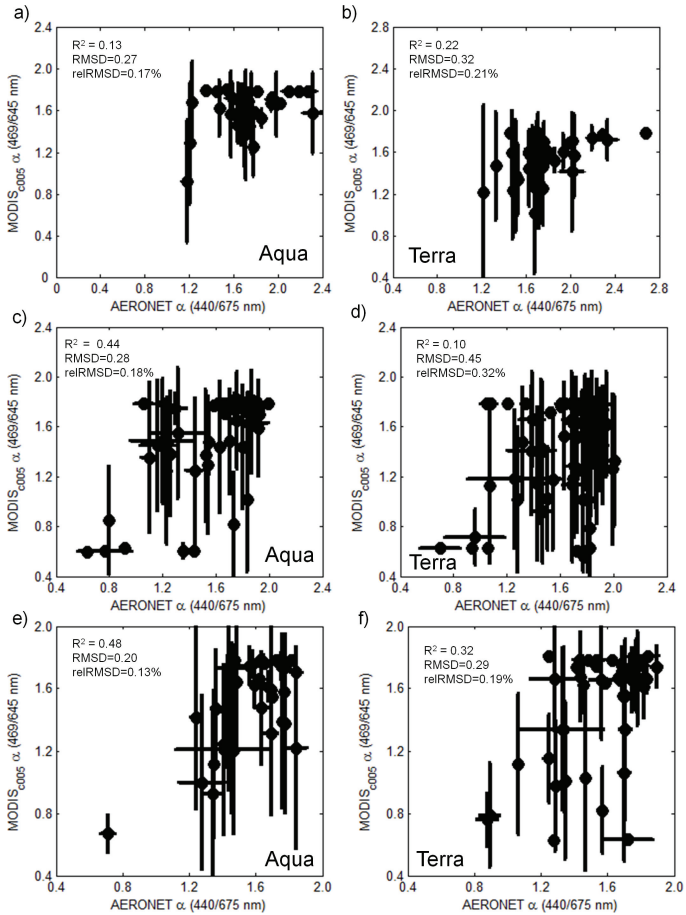

Fig. 5. Same as Fig. 4 but for a comparison of MODIS c005 and AERONET α for the wavelength pairs 469/645 and 440/675 nm, respectively.

AMTD
5, 2363–2393, 2012

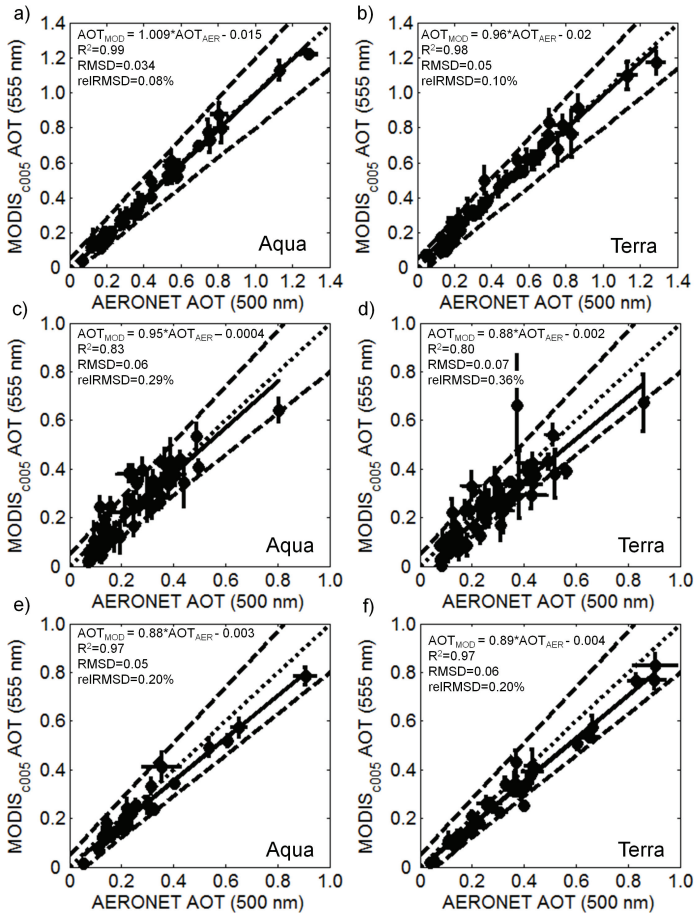

Fig. 6. Same as Fig. 4 but for a comparison of MODIS c005 and AERONET AOT at 555 and 500 nm, respectively.

AMTD
5, 2363–2393, 2012

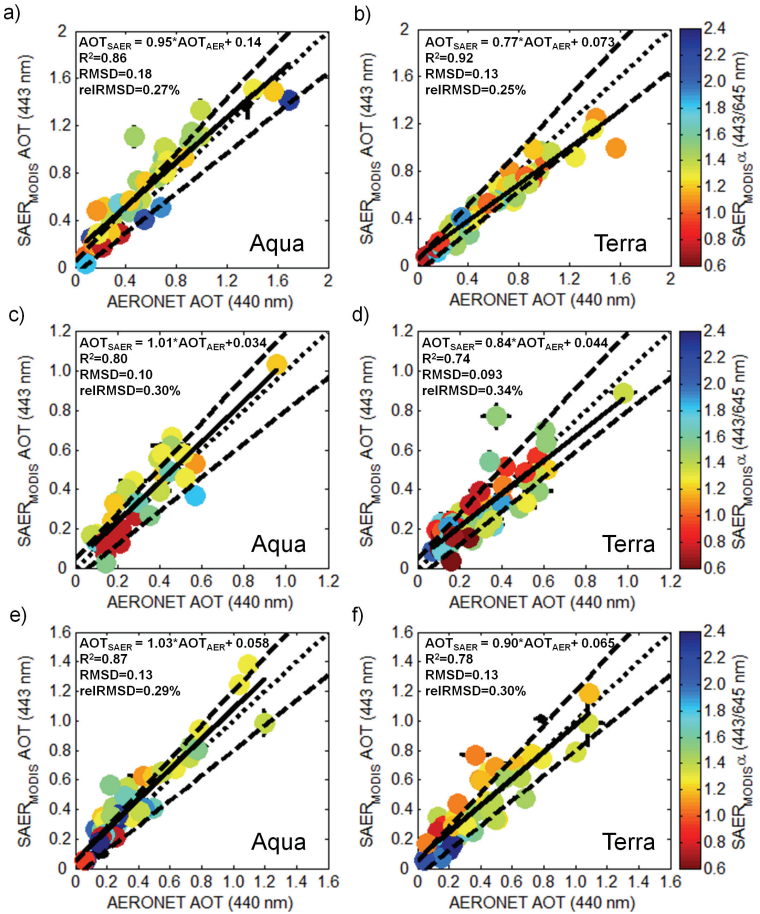

Fig. 7. Same as Fig. 4 but for a comparison of $SAER_{MODIS}$ and AERONET AOT at 443 and 440 nm, respectively. The color coding refers to α as obtained with $SAER_{MODIS}$ for the wavelength pair 443/645 nm.

AMTD
5, 2363–2393, 2012

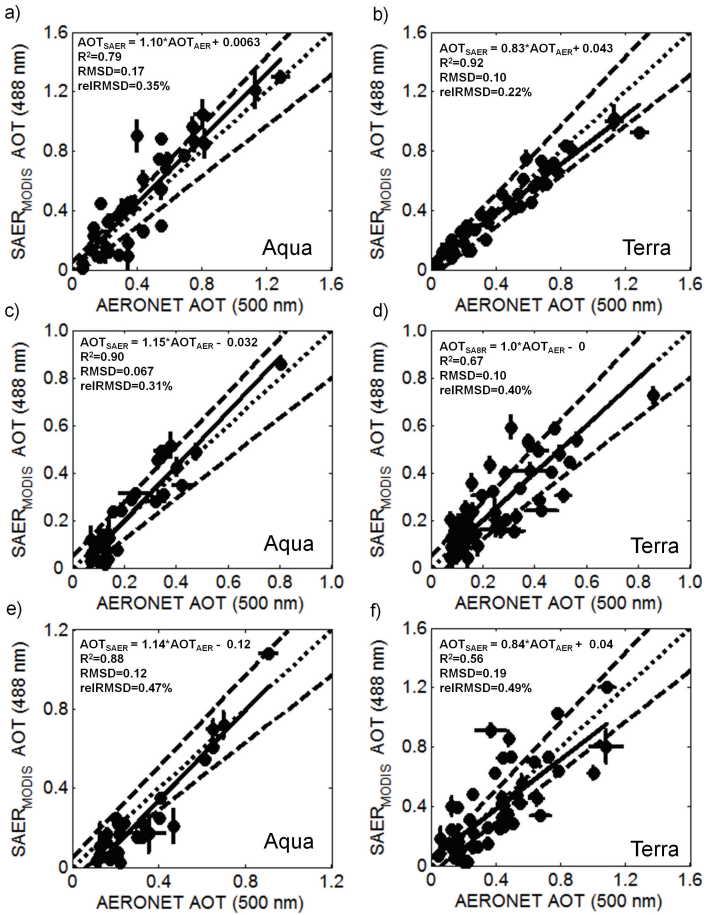

Fig. 8. Same as Fig. 4 but for a comparison of $SAER_{MODIS}$ and AERONET AOT at 488 and 500 nm, respectively.

AMTD
5, 2363–2393, 2012

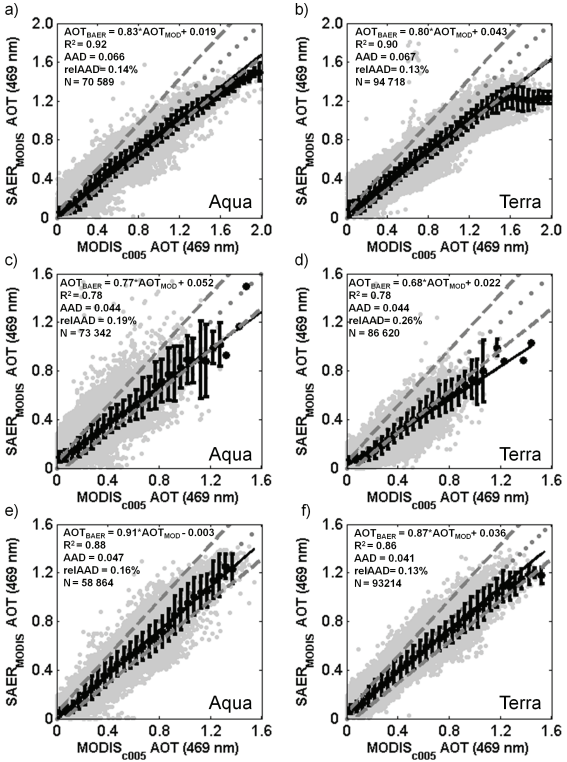

Fig. 9. Pixel-by-pixel (10 km) comparison of SAER and MODIS c005 AOT over land surfaces in Europe. Black dots and error bars denote mean AOT values in intervals of 0.05 and the corresponding one standard deviation, respectively. The solid black, and the dashed and dotted grey lines represent linear fits, expected uncertainties for one standard deviation of the MODIS c005 aerosol retrievals, and 1-to-1 line, respectively.

AMTD
5, 2363–2393, 2012

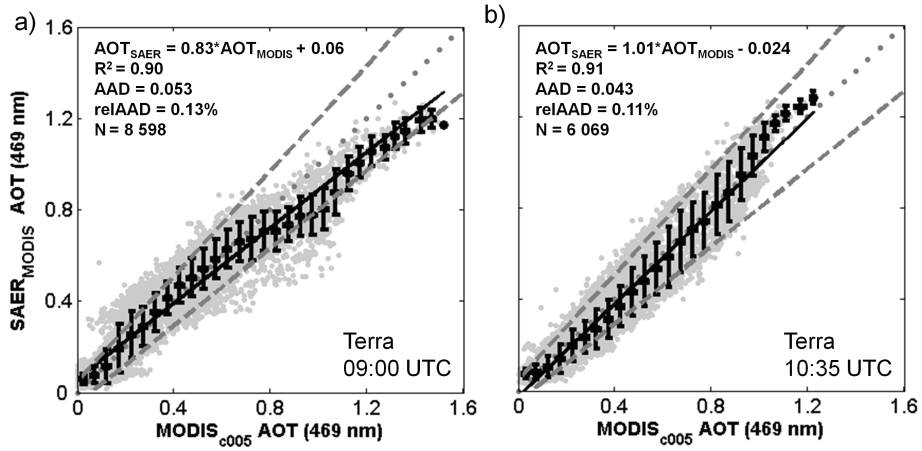

Fig. 10. Same as Fig. 9 but only for two Terra overpasses over Europe on 1 April 2007, at **(a)** 09:00 UTC and **(b)** 10:40 UTC.

AMTD
5, 2363–2393, 2012